forum acusticum 2026
8-12 September · Graz, Austria

DESIGN OF A PHASE GRADIENT METAMATERIAL WITH PERFORATED FOAMS

Adrien Guthapfel[1,3], Hervé Denayer[1,3], Edwin Reynders[2,3], Elke Deckers[1,3]

[1] *Department of Mechanical Engineering, KU Leuven, Belgium*
[2] *Department of Civil Engineering, KU Leuven, Belgium*
[3] *Flanders Make, Heverlee, Belgium*

Abstract

In recent years, phase-gradient metamaterials have attracted significant attention for their ability to steer incident waves. Their behavior follows the generalized Snell's law, which links reflected and transmitted wave directions to the phase gradient of their coefficients along the surface. By imposing a linear phase profile, reflected waves can be converted into surface waves and subsequently suppressed using an absorbing layer, enabling high-performance absorption.

In practice, these metamaterials consist of periodic arrays of discrete cells incorporating porous layers, space-coiling geometries, or locally resonant elements, each designed to provide a targeted phase response. Recent studies seek to achieve strong absorption by controlling reflection phase gradient, but achieving these profiles often results in bulky designs.

This study proposes a metamaterial based on highly tortuous perforated foam, typically used outdoors and resembling a double-porosity material. Its tunable perforation parameters and excellent low-frequency absorption make it a promising candidate for generating the required phase gradients within a subwavelength structure. The paper presents the complete design process, from phase-control analysis through perforation tuning to metamaterial optimization, including foam-property and geometry selection, and a sensitivity analysis assessing amplitude-related deviations between theoretical and actual material properties.

Keywords: *phase gradient metamaterial, sound absorption, perforated foam*

Corresponding author: *adrien.guthapfel@kuleuven.be.*

1. Introduction

Phase gradient metamaterials (PGMs) have recently emerged as a highly promising solution for sound absorption due to their ability to suppress the reflection of incident waves through the generalized Snell's law. This can be achieved by periodically arranging cells composed of porous layers, space-coiling structures, or locally resonant elements. Owing to their ability to manipulate the direction of reflected waves, PGMs can also be employed in other applications, such as acoustic cloaks and acoustic lenses [1].

In conventional PGMs composed of alternating layers of air and porous absorbing foam Fig. 1, the required phase gradient is achieved by varying both the thickness and the position of the foam layers. However, such an approach generally results in bulky structures. This paper proposes an alternative design based on perforated porous foam, whose acoustic properties can be tailored through the geometric characteristics of the perforations. This type of double-porosity material enables significant variations in acoustic behavior through geometric modifications alone, without altering its overall thickness. Consequently, the local phase response at the metamaterial surface can be adjusted without increasing the total thickness of the structure, enabling the realization of compact PGMs. An optimization framework for the design of such metamaterials is also presented.

The paper is organized as follows. First, the ability of the perforated foam to modify its acoustic properties as a function of its geometry is investigated, together with the resulting variations in the reflection coefficient of an individual unit cell. Particular attention is given to the local acoustic response of each cell. Second, the assembly of individual cells into a phase gradient metamaterial is presented through the description of the proposed PGM design algorithm. Finally, the resulting optimized PGM configurations are discussed.

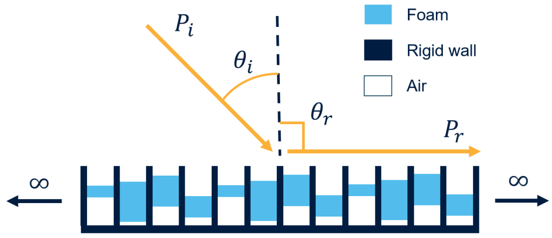

Figure 1: Representation of a PGM with P_i and P_r respectfully the incident and reflected pressures and θ_i, θ_r the angles of incidence and reflection.

2. Phase manipulation via perforated foam

2.1. Foam characteristics variability

The perforated foam investigated in [2] exhibits a high absorption performance in the 600-800 Hz frequency range with a thickness of only $L = 4$ cm, making it a particularly compact solution relative to its absorption peak frequency. The material is characterized by four tunable geometric parameters: the wall thickness between adjacent cells t, the cell radius C_r, the perforation radius r_p, and the spacing between neighboring perforations d_p Fig. 2. These parameters govern the effective acoustic properties of the foam and therefore provide a means of tailoring its local phase response.

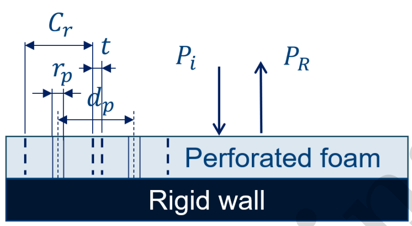

Figure 2: Representation of the perforated foam with its characteristics with t the cell wall thickness, C_r the cell radius, r_p the perforation radius, d_p the distance between perforations.

In [2], the acoustic behavior of the perforated foam is modeled using the Johnson-Champoux-Allard (JCA) model. The model relies on a set of macroscopic parameters, namely the porosity ϕ, the high-frequency tortuosity limit τ^{∞}, the viscous characteristic length Λ, the thermal characteristic length Λ', and the airflow resistivity σ. Each of these JCA parameters is expressed as a function of the foam geometry. However, for most parameters, these relationships are empirical and are available only for a limited number of data points. Consequently, a regression model is required to continuously describe the acoustic behavior of the foam across the design space. Because of the sparse nature of the available dataset, a probabilistic approach based on Gaussian process regression [3] is adopted such that, for instance, $\phi = \mathcal{GP}(t, C_r, r_p, d_p)$. This approach is also adopted for the other JCA parameters τ^{∞},Λ,Λ'. The air flow resistivity σ is the only parameter with an empirical law found in [2]. Once the they have been estimated, the equivalent acoustic properties of the material, namely the effective density ρ_{eq} and the equivalent bulk modulus K_{eq}, can be derived. [4]

$$\rho_{eq}(\omega) = \frac{\tau_\infty \rho_0}{\phi}\left[1 + \frac{\sigma\phi}{i\omega\rho_0\tau_\infty}\sqrt{1 + \frac{4\rho_0^2\eta\omega}{\sigma^2 - \Lambda^2\phi^2}}\right], \tag{1}$$

$$K_{eq}(\omega) = \frac{\gamma P_0/\phi}{\gamma - (\gamma-1)\left[1 - i\frac{8\kappa}{\Lambda^2 C_p\rho_0\omega}\sqrt{1 - i\frac{\Lambda^2 C_p\rho_0\omega}{16\kappa}}\right]^{-1}}, \tag{2}$$

where ρ_0 denotes the density of air, η its dynamic viscosity, P_0 the atmospheric pressure, γ the ratio of specific heats, C_p the specific heat capacity at constant pressure, and κ the thermal conductivity. From these equivalent material properties, the equivalent characteristic impedance Z_c can be determined, together with the associated complex wavenumber. These quantities fully describe the propagation of acoustic waves within the porous medium and constitute the basis for predicting the reflection, transmission, and absorption behavior of the perforated foam.

$$Z_c = \sqrt{K_{eq}\rho_{eq}}, \quad k_f = \omega\sqrt{\frac{\rho_{eq}}{K_{eq}}}. \tag{3}$$

2.2. Reflection coefficient of a cell

To construct the proposed PGM, we focus on the reflection coefficient at the surface of each unit cell, and more specifically on its amplitude and phase. The overall set of reflection coefficients can be expressed as

$$R_g = \{R_1, R_2, ..., R_N\} = |r|e^{j\{\Phi_1,\Phi_2,...,\Phi_N\}}, \tag{4}$$

with N the number of cells in a period, R_i the coefficients of reflection on top of each cell, $|r|$ the amplitude and Φ_i their phase.

For the phase gradient to operate effectively as mentionned in [5], two conditions must be satisfied: the reflection amplitude should remain approximately constant across all unit cells, and the reflection phase should be uniformly distributed over the interval $[0, 2\pi]$ according to the number of cells composing the metamaterial. Failure to satisfy these requirements may lead to deviations from the ideal response, resulting in reduced wavefront control and degraded absorption performance.

To design the PGM, the reflection coefficient of each unit cell must first be determined independently and then assembled according to the targeted amplitude and phase distributions. For the computation of these coefficients, only plane-wave propagation within each cell is assumed as in Fig. 3. Under this assumption, the Transfer Matrix Method (TMM) can be employed to model wave propagation through the multilayer structure and to evaluate the reflection coefficient at the cell surface :

$$R_c = e^{-2jk_a l_1} \frac{e^{jk_f L}(Z_f - Z_a)A + e^{-jk_f L}(Z_f + Z_a)B}{e^{jk_f L}(Z_f + Z_a)A + e^{-jk_f L}(Z_f - Z_a)B}, \quad (5)$$

$$A = 2Z_a \cos(k_a l_2) + 2jZ_f \sin(k_a l_2), \quad (6)$$

$$B = 2Z_a \cos(k_a l_2) - 2jZ_f \sin(k_a l_2). \quad (7)$$

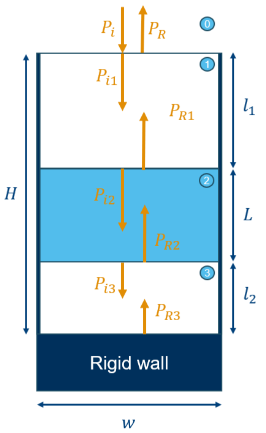

Figure 3: Representation of a cell with P_{in}, P_{Rn}, the incident and reflected pressure waves in each of the layers of the cell. L is the thickness of the foam, H the thickness of the cell and l_1,l_2, the thicknesses of the layers of air.

3. Design process

3.1. Goal and Application

To determine the most appropriate PGM configuration, it is first necessary to clearly define the intended application of the system as well as the associated design constraints. These considerations make it possible to identify key specifications, such as the maximum admissible thickness of the metamaterial and the frequency range of interest. In the present study, the proposed PGM is designed as a narrowband absorber targeting a specific operating frequency, denoted by f_a.

As a representative example, we consider the perforated foam investigated in [2], for which the developed models predict absorption peaks exceeding $\alpha > 0.8$ around $f_a \approx 650$ Hz with a uniform thickness of only $L = 2.5$ cm, corresponding to approximately $\lambda/21$. In this work, the same thickness is adopted for the PGM, namely $H = 2.5$ cm, while targeting a lower operating frequency of $f_a = 500$ Hz, yielding a subwavelength thickness of approximately $H = \lambda/27$.

The metamaterial thickness and the target frequency constitute the primary design constraints. Nevertheless, additional parameters, such as the unit-cell width w and the periodicity distance d of the unit-cell, must also be specified. The cell widths may, in principle, be adjusted to compensate for imperfections in the phase profile and thereby mitigate deviations from the ideal response. However, for this study, all unit cells are assumed to have identical widths, such that $w_i = d/N$ where N denotes the total number of cells within a period. The periodicity distance d is directly related to the phase-gradient mechanism. To ensure the conversion of reflected waves into surface waves, the periodicity must remain smaller than half the acoustic wavelength in air. By selecting $d = 6$ cm, this requirement is satisfied at the target frequency, thereby enabling the desired wave manipulation regime.

3.2. Assembly and phase profile creation

The PGM is constructed by assembling individual cells side to side horizontally according to their reflection coefficients to create the whole unit-cell. The first step consists of generating a database of candidate cells with varying properties: different perforated foam configurations characterized by the geometric parameters (t, C_r, d_p, r_p), together with the foam thickness L and its position within the unit cell, y_f. This database constitutes the set of elementary building blocks from which the PGM can be designed.

The phase and magnitude of the reflection coefficient associated with each candidate cell can be conveniently visualized using a polar representation, as illustrated in Fig. 5. Given the imposed design constraints, such a representation provides an initial assessment of the feasibility of realizing a PGM and identifies the phase profiles that can realistically be achieved. In general, high reflection magnitudes are associated with a limited phase coverage, making the realization of a complete phase gradient more challenging. Conversely, lower reflection magnitudes typically allow a wider phase range, thereby enabling a finer discretization of the phase gradient using more than two unit cells.

The design procedure can be summarized as follows. First, the number of unit cells per period is selected. The candidate cells are then grouped according to the magnitude of their reflection coefficient, $|r|$, in order to satisfy the requirement of a nearly uniform reflection amplitude across the PGM surface. An admissible amplitude tolerance must therefore be defined to ensure a sufficiently consistent surface impedance and to avoid performance degradation caused by excessive amplitude variations.

Second, each amplitude group is subdivided according to the phase of the reflection coefficient, denoted by Φ_c. For a given number of cells N, the phase interval $[0, 2\pi]$ is divided into N equal segments corresponding to the desired phase states. Candidate cells are then assigned to these phase intervals according to their respective phase responses. All possible PGM configurations are generated by selecting one cell from each phase interval, thereby constructing discrete approximations of the target phase gradient. As a result, a collection

of candidate PGMs is obtained, each characterized by a specific reflection amplitude and phase-gradient discretization.
Third, using the analytical model described in [5], the global reflection coefficient and the corresponding absorption coefficient at the target frequency can be computed for each candidate PGM. A selection criterion is then applied, retaining only the configurations satisfying $\alpha > 0.9$ at the design frequency. Finally, the procedure is repeated for different numbers of unit cells per period, with $N \in [2, 5]$, and the absorption performance of the selected PGMs is evaluated over the frequency range $f \in [20, 5000]$ Hz. The design showcasing the best broadband absorption amongst the pool of created PGMs is ultimately chosen as the configuration exhibiting the best broadband absorption performance over the frequency range under consideration.

3.3. Impact of amplitude variation

For a PGM, the magnitude of the reflection coefficient is ideally required to remain constant across all unit cells. However, depending on the specific cells selected to construct the metamaterial, variations in the overall performance may still arise. Consequently, within the proposed design procedure, it is necessary to define an amplitude interval over which different reflection coefficients can be considered equivalent and therefore grouped together.
To establish this interval, the reflection coefficient of each unit cell is expressed as

$$R_c = (|r| + \delta r)e^{j\Phi}, \tag{8}$$

where δr represents the local amplitude variation associated with a given unit cell. This variation is modeled as a random variable following a uniform distribution over the interval $[r - \Delta r, r + \Delta r]$. The objective is to generate a sufficiently large number of theoretical PGM realizations in order to evaluate the impact of reflection-magnitude fluctuations on the overall performance of the metamaterial. More specifically, this approach enables the assessment of worst-case scenarios and determines whether a prescribed amplitude variance leads to a significant degradation of the absorption performance. To compare the different realizations, the Root Mean Square Error (RMSE) is employed as a measure of the deviation between the target reflection magnitude r and the actual reflection magnitudes assigned to the unit cells. The RMSE is defined as

$$RMSE = \sqrt{\frac{1}{N}\sum_i (\delta r_i)^2}. \tag{9}$$

In Fig. 4, a reference reflection magnitude of $|r| = 0.5$ is considered, which is higher than the values encountered for the PGMs investigated in this work. In other cases, the PGM could have higher values of amplitude which would need a smaller interval to use. As the reflection magnitude increases, variations in its

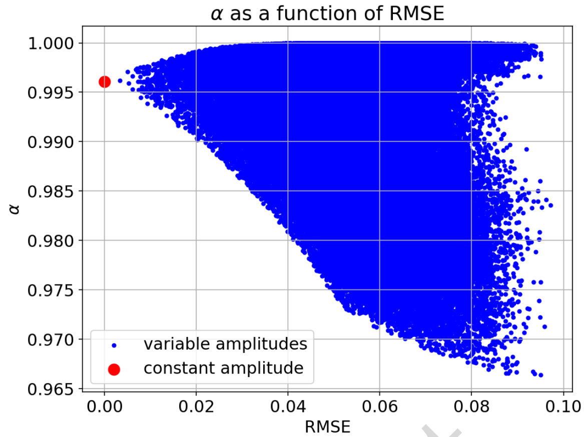

Figure 4: Variation of the absorption of a 4 cell PGM depending on the Root Mean Square Error in the amplitude with $|r| = 0.5$, $\Delta r = 0.1$.

value are expected to have a more pronounced impact on the absorption performance of the metamaterial. The maximum variation, $\Delta r = 0.1$, corresponds to the tolerance adopted in the proposed PGM design algorithm. It can be observed that the absorption performance remains largely unaffected by these fluctuations, with the lowest recorded value approaching $\alpha = 0.965$. This result remains highly satisfactory and well above the minimum absorption threshold imposed during the design process.
In principle, it would be possible to assemble the cells using a purely combinatorial approach by evaluating every possible PGM configuration generated from the available unit-cell database. However, the proposed grouping strategy significantly reduces the number of candidate configurations and, consequently, the computational cost, while remaining consistent with the underlying physical requirements of the phase-gradient mechanism. Similarly, a finer discretization of the phase-gradient intervals could be introduced to further reduce the number of admissible configurations and streamline the optimization procedure.

3.4. Resulting models

In Fig. 5, the best-performing configurations identified by the optimization algorithm are presented together with the selected unit cells. Owing to the phase-grouping strategy adopted during the design process, no sufficiently efficient configurations could be found for PGMs composed of three or five unit cells per period. Consequently, only two candidate PGM designs were retained for further analysis.
A first observation is that configurations exhibiting a low reflection magnitude are naturally favored, since minimizing the reflected energy is essential for maximizing acoustic absorption. Nevertheless, the selected designs do not correspond to the cells with the lowest reflection magnitudes available in the database. This highlights the crucial role played by the phase gradient itself in the overall performance of the meta-

material. A second noteworthy observation concerns the non-uniformity of the phase gradients obtained for both designs. Indeed, the wavefront manipulation mechanism induced by the phase gradient appears to be sufficiently robust to maintain its effectiveness even when the phase and amplitude distributions deviate from the ideal theoretical profile.

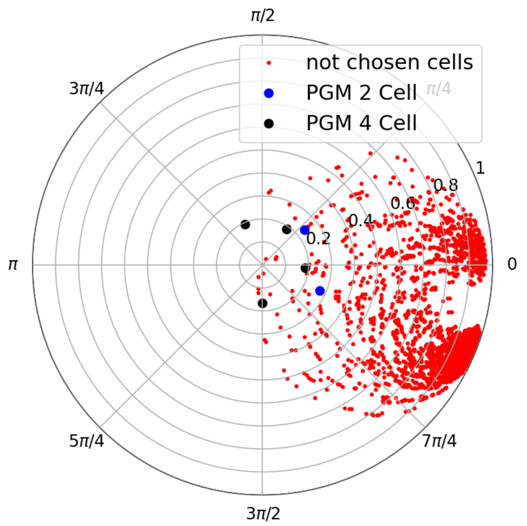

Figure 5: Distribution of the coefficient of reflection of each cell on a polar graph with the chosen profiles, $f_a = 500$Hz and $H = 0.025$m. The radius is the amplitude $|r|$, and the angle is its phase Φ

The absorption results are presented in Fig. 6, where the two optimized PGMs are compared with a uniform perforated foam layer of identical thickness, $L = H = 2.5$ cm, specifically designed to exhibit its absorption peak at $f_a = 500$ Hz. At the target frequency, the uniform foam exhibits significantly lower performance, with an absorption coefficient slightly above 0.65. In contrast, both PGMs achieve absorption coefficients exceeding 0.9, while the four-cell configuration approaches near-perfect absorption.
These results indicate that increasing the number of unit cells per period improves the discretization of the desired phase gradient, allowing the resulting phase profile to approximate more closely an ideal linear distribution. Consequently, enhanced absorption performance is obtained. The main limitation of the proposed designs, however, lies in their inherently narrowband behavior, as high absorption levels are achieved only within a relatively limited frequency range around the target frequency.

4. Conclusion

This study demonstrates the strong potential of perforated porous foams for the implementation of phase-gradient metamaterials. By tailoring the acoustic properties of the foam through its perforation geometry, a wide range of reflection-coefficient magnitudes and phases can be achieved at the surface, enabling the realization of the desired phase profiles.

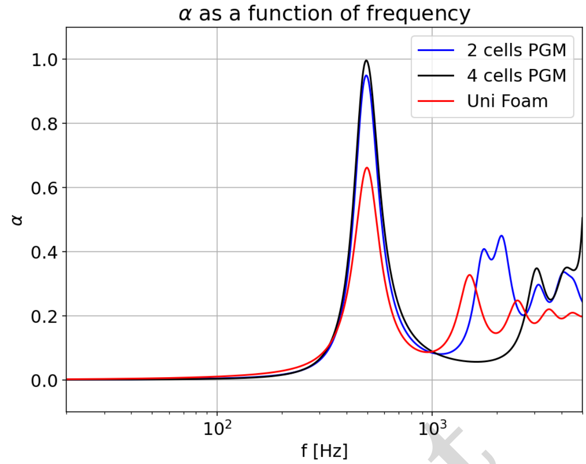

Figure 6: Absorption α of the two PGMs profiles found by the program and the uniform perforated foam designed for $f_a = 500$Hz as a function of the frequency.

The proposed design algorithm successfully identified high-performance PGM configurations that satisfy the imposed constraints. Furthermore, the resulting metamaterials provide a significant improvement over the reference uniform foam, despite operating with a reduced relative thickness, from $L = \lambda/21$ for the original foam absorber to $H = \lambda/27$ for the optimized PGM.
These findings establish a promising foundation for future developments of porous phase-gradient metamaterials. Potential extensions include the consideration of alternative boundary conditions and excitation scenarios, the implementation of more advanced optimization strategies involving multiple layers within a single cell, and the exploration of novel design approaches aimed at achieving broadband absorption while maintaining the compact characteristics of the proposed structures.

5. Acknowledgements

This research was partially supported by Flanders Make, the strategic research centre for the manufacturing industry. Internal Funds KU Leuven are gratefully acknowledged for their support.

References

[1] J. Guo, Y. Fang, R. Qu, and X. Zhang, "Development and progress in acoustic phase-gradient metamaterials for wavefront modulation," *Materials Today*, vol. 66, pp. 321–338, 2023.

[2] B. V. Damme, T. Cavalieri, C.-T. Nguyen, and C. Perrot, "Enhancement of the sound absorption of closed-cell mineral foams by perforations: Manufacturing process and model-supported adaptation," *Materials Design*, vol. 249, no. 113540, 2025.

[3] E. Schulz, M. Speekenbrink, and A. Krause, "A tutorial on gaussian process regression: Modelling,

exploring, and exploiting functions," *Journal of Mathematical Psychology*, vol. 85, pp. 1–16, 2018.

[4] M. J. Cops, J. G. McDaniel, E. A. Magliula, D. J. Bamford, and M. Berggren, "Estimation of acoustic absorption in porous materials based on visco-thermal boundary layers modeled as boundary conditions," *Journal of Acoustic Society of America*, vol. 148, no. 3, pp. 1624–1635, 2020.

[5] Z. Zhang, H. Denayer, C. Claeys, W. Desmet, and E. Deckers, "Theoretical analysis of phase gradient combinations in acoustic metamaterials using fourier decomposition model," *Journal of Sound and Vibration*, vol. 636, no. 119788, 2026.